Acta Oceanol. Sin., 2021, Vol. 40, No. 2, P. 65–80
https://doi.org/10.1007/s13131-021-1759-5
http://www.hyxb.org.cn
E-mail: hyxbe@263.net

Characteristics and origins of middle Miocene mounds and channels in the northern South China Sea

Yufeng Li[1, 2, 3, 4], Gongcheng Zhang[5], Renhai Pu[2, 3*], Hongjun Qu[2, 3], Huailei Shen[5], Xueqin Zhao[1]

[1] School of Environment and Resource, Southwest University of Science and Technology, Mianyang 621010, China

[2] State Key Laboratory of Continental Dynamics, Xi'an 710069, China

[3] Department of Geology, Northwest University, Xi'an 710069, China

[4] Key Laboratory of Marine Mineral Resources, Ministry of Natural Resources, Guangzhou 510075, China

[5] CNOOC Research Institute Co., Ltd., Beijing 100028, China

Received 1 October 2019; accepted 25 May 2020

Abstract

Numerous elongated mounds and channels were found at the top of the middle Miocene strata using 2D/3D seismic data in the Liwan Sag of Zhujiang River Mouth Basin (ZRMB) and the Beijiao Sag of Qiongdongnan Basin (QDNB). They occur at intervals and are rarely revealed by drilling wells in the deepwater areas. Origins of the mounds and channels are controversial and poorly understood. Based on an integrated analysis of the seismic attribute, palaeotectonics and palaeogeography, and drilling well encountering a mound, research results show that these mounds are dominantly distributed on the depression centres and/or slopes of the Liwan and Beijiao sags and developed in a bathyal sedimentary environment. In the Liwan and Beijiao sags, the mounds between channels (sub) parallel to one another are 1.0–1.5 km and 1.5–2.0 km wide, 150–300 m and 150–200 m high, and extend straightly from west to east for 5–15 km and 8–20 km, respectively. Mounds and channels in the Liwan Sag are parallel with the regional slope. Mounds and channels in the Beijiao Sag, however, are at a small angle to the regional slope. According to internal geometry, texture and external morphology of mounds, the mounds in Beijiao Sag are divided into weak amplitude parallel reflections (mound type I), blank or chaotic reflections (mound type II), and internal mounded reflections (mound type III). The mounds in Liwan Sag, however, have the sole type, i.e., mound type I. Mound type I originates from the incision of bottom currents and/or gravity flows. Mound type II results from gravity-driven sediments such as turbidite. Mound type III is a result of deposition and incision of bottom currents simultaneously. The channels with high amplitude between mounds in the Beijiao and Liwan sags are a result of gravity-flow sediments and it is suggested they are filled by sandstone. Whereas channels with low-mediate amplitudes are filled by bottom-current sediments only in the Beijiao Sag, where they are dominantly composed of mudstone. This study provides new insights into the origins of the mounds and channels worldwide.

Key words: South China Sea, middle Miocene, channels and mounds, contour currents

Citation: Li Yufeng, Zhang Gongcheng, Pu Renhai, Qu Hongjun, Shen Huailei, Zhao Xueqin. 2021. Characteristics and origins of middle Miocene mounds and channels in the northern South China Sea. Acta Oceanologica Sinica, 40(2): 65–80, doi: 10.1007/s13131-021-1759-5

1 Introduction

The Zhujiang River Mouth Basin (ZRMB) and Qiongdongnan Basin (QDNB) (together abbreviated as ZRMB-QDNB) are located in the northern South China Sea (SCS). There are a wide variety of geological phenomena in the northern SCS, some of which are various similarly mounded seismic reflection bodies, such as sand intrusion mounds (Yang et al., 2014), mud diapirs or mud volcanoes (Meng et al., 2012), volcanoes dome (Pu et al., 2013; Zhang et al., 2013), carbonate reefs (Chen et al., 2011; Zhang et al., 2011; Wang et al., 2015), sediment waves related to bottom currents (Zhao et al., 2013), contourite drifts (Chen et al., 2016; Sun et al., 2017), lime-mud mounds (Andresen et al., 2009), and remnant mounds originated from the bottom current incision (Sun et al., 2016). In recent years, the modern channels formed by contour (bottom) currents are documented in previous studies (Chen et al., 2014, 2016; Gong et al., 2016; Sun et al., 2017), some of which can be traced back to the early late Miocene in the northern SCS.

In recent years, pervasive mounds are found in the middle Miocene in the ZRMB-QDNB, which attracts much attention from geologists. In the academic circle, most geologists widely accept a viewpoint that it is an important period of reef development in the middle Miocene in the northern SCS (Wu et al., 2014; Shao et al., 2017). Furthermore, the middle Miocene Liuhua field reefs containing oil and gas are found in the Dongsha Uplift in the ZRMB (Ma et al., 2010). In the Liwan and Beijiao sags, mounds and channels are pervasively identified using both the 2D and 3D seismic surveys in the middle Miocene. Based on the shape, property, and locations of mounded seismic reflections, Wu et al. (2009), Zhang et al. (2011), Huang et al. (2012), and Yi

Foundation item: The National Science and Technology Major Project of China under contract Nos 2011ZX05025-006-02 and 2016ZX05026-007; the National Natural Science Foundation of China under contract Nos 41390451 and 41672206; the Doctoral Fund of Southwest University of science and technology under contract No. 18zx711901; the Fund of Key Laboratory of Marine Mineral Resources of Ministry of Natural Resources under contract No. KLMMR-2018-B-07.

*Corresponding author, E-mail: purenhai@126.com

et al. (2012) suggest that the mound reflections in the Beijiao Sag might be carbonate reefs. However, mainly based on 2D seismic data and especially after a mud mound encountered by a drilling well, these mound reflections are interpreted as other origins such as sediment waves or contourite drift (Zhao et al., 2013), and mud mounds originated from the combined results of gravity flow and bottom current (Tian et al., 2015). Furthermore, based on paleotectonics, paleogeography, and seismic mounded reflection geometries, mud diapir and mud volcanoes resulting in the mounds have been excluded in the Beijiao Sag (Zhao et al., 2013; Tian et al., 2015). In the Liwan Sag, however, the mounds and channels are few documented in previous studies.

In this paper, the authors indicate these interpretations about the mounds and channels are a shortage of overwhelming evidence. Based on the newly acquired drill bore data (YLx), interpretation of 2D and 3D seismic data in combination with an analysis of the sediment environment and paleoceanography in the study areas, this paper attempts to (1) characterize the geomorphologic and seismic attribute features of these mound and channel structures, (2) unravel their possible origins, e.g, turbidity-flow and/or bottom-current deposition or erosion, and (3) illustrate their importance. Although deep-water deposition system, currently, remains poorly understood, this study may improve the overall understanding of deep-water sedimentation processes in the northern SCS.

2 Geological and oceanographical context

2.1 *Tectonic setting and sedimentary environment evolution*

The SCS is one of the largest passive continental margin seas in the Western Pacific Ocean (Ru and Pigott, 1986). ZRMB-QDNB are bounded by Taiwan to the east, Hainan Island and Hong Kong to the north, Yinggehai Basin to the west, Xisha Massif to the south (Fig. 1). They consist of the tectonic units of the Northern Uplift, Northern Sag, Central Uplift, Southern Sag, and Southern Uplift from north to south (Fig. 2). Both of the ZRMB and QDNB are the Cenozoic basins, which are developed on a Mesozoic igneous basement. They mainly experience three tectonic evolution stages of rifting, thermal subsidence, and accelerated thermal subsidence (Zhang et al., 2009; Zhang, 2010; Tian et al., 2015) (Table 1). Basin fills are in response to the three tectonic evolutionary stages. The depositional environment transforms from alluvial to lacustrine, onshore to neritic and shelf-slope to abyssal environments from the Paleocene to the present day (Xie et al., 2006; Tian et al., 2015; Liu et al., 2016).

Nine stratigraphic horizons/surfaces from Eocene to Pleistocene have been seismically identified (Figs 3 and 4) and were tied to well (YLx) in the study areas. They correspond to Tg (53.5 Ma), T80 (32.0 Ma), T70 (29.3 Ma), T60 (23.3 Ma), T50 (15.5 Ma), T41 (13.8 Ma), T40 (11.6 Ma), T30 (5.5 Ma), and T20 (1.9 Ma) (Xie et al., 2006; Chen et al., 2014). The mounds are within the T41–T40 seismic horizons (13.8–11.6 Ma), which correspond to the upper middle Miocene Meishan Formation (Table 1). The channels are distributed between the mounds at the bottom of the upper Miocene.

2.2 *Oceanographic setting*

Due to the influence of the East Asia monsoon and intrusion of Kuroshio current, ocean currents in the northern SCS are still controversial and complex (Xue et al., 2004) (Fig. 1). In the nearby Luzon Strait, the ocean circulation can be mainly divided

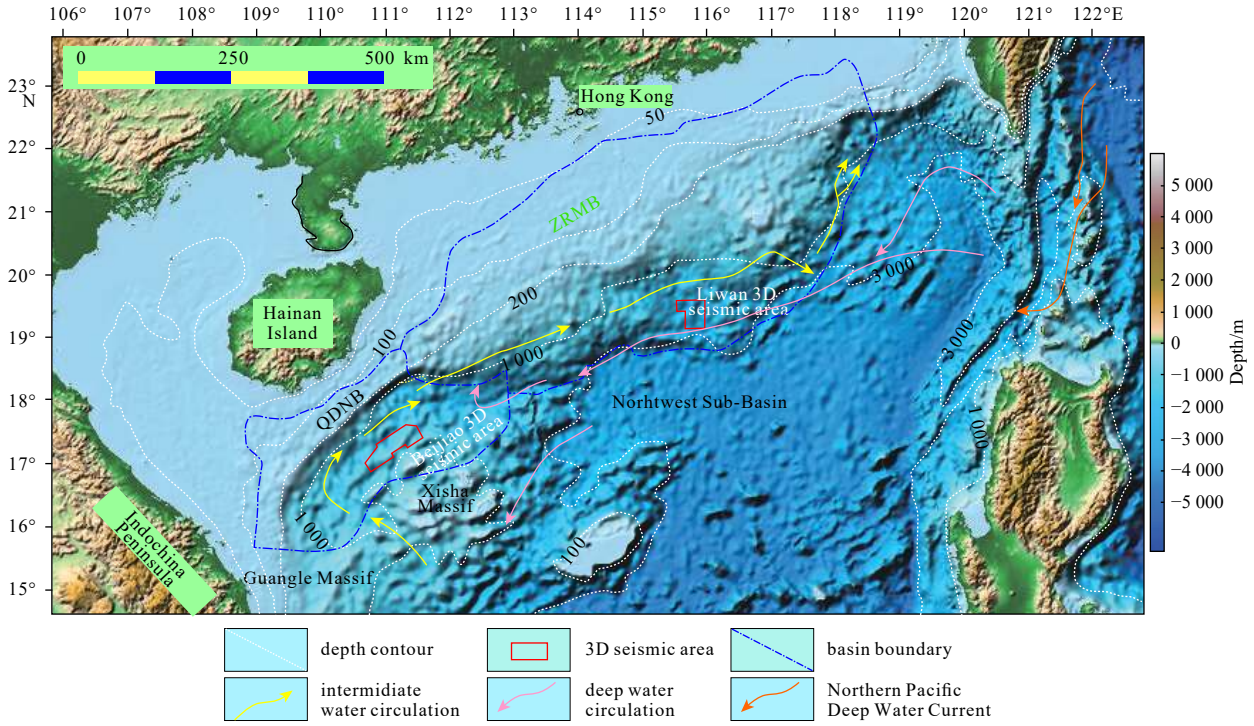

Fig. 1. Bathymetric map from the northern South China Sea (SCS). The yellow solid arrows are the inferred intermediate water circulation (modified from Zhu et al. (2010); Chen et al. (2014) and Sun et al. (2017)); the pink solid arrows represent the assumed deep water circulation pathways in the northern SCS (modified from Shao et al. (2007), Zhu et al., (2010) and Chen et al., (2014)); the jacinth solid arrows are pathways for the Northern Pacific Deep Water Current into the SCS via the Bashi Channel and the Luzon Strait (modified from Gong et al. (2012) and Tian et al. (2015)). QDNB means Qiongdongnan Basin; ZRMB means Zhujiang River Mouth Basin.

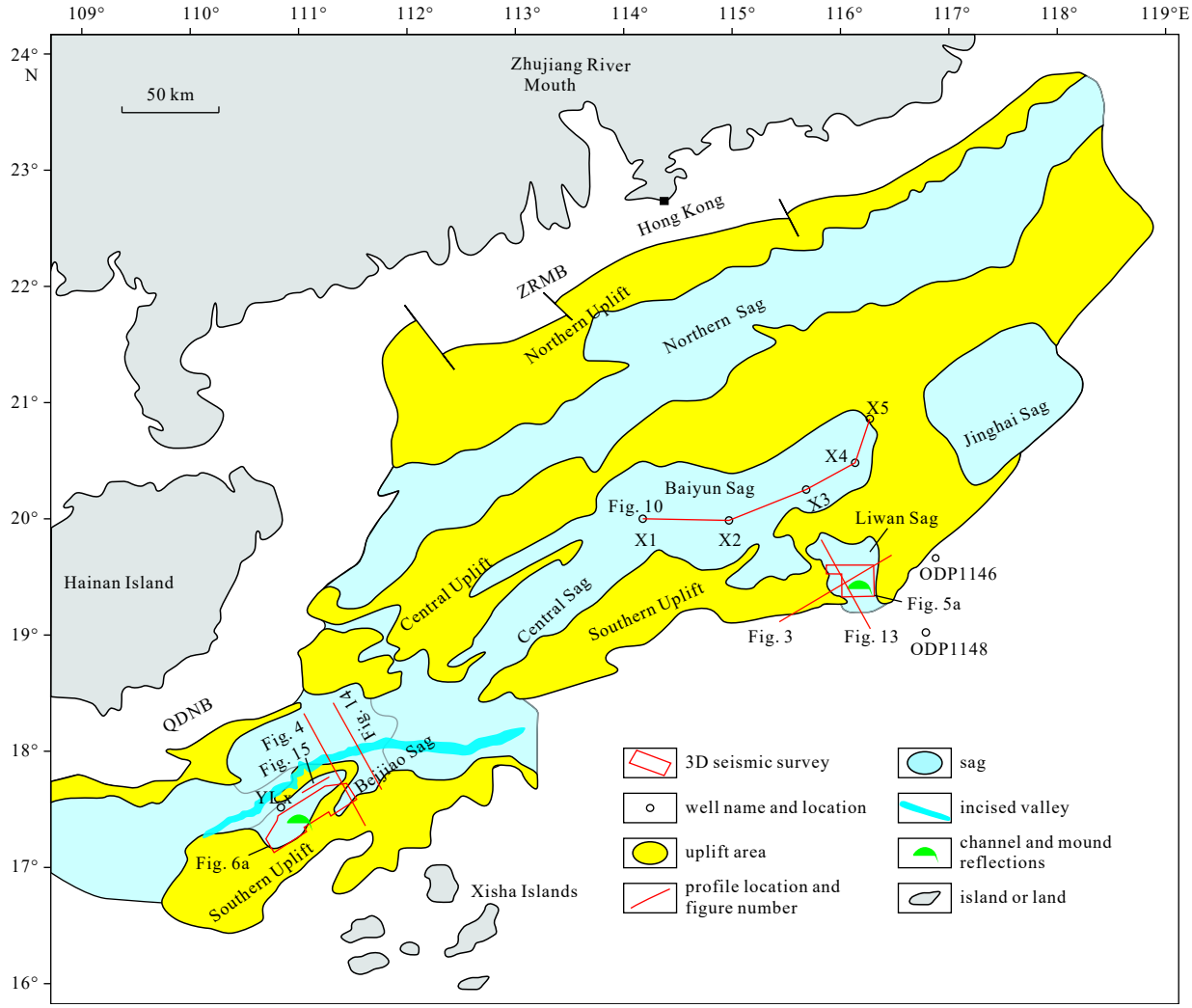

Fig. 2. Tectonic units in the ZRMB-QDNB and the locations of the middle Miocene channel and mound reflections.

Table 1. Absolute ages and basin evolution stages corresponding to the Miocene channels and mounds in the deep-water area in the ZRMB-QDNB (modified from Zhang et al. (2009) and Zhang (2010))

Stratigraphy				Lithological stratigraphy of QDNB	Lithological stratigraphy of ZRMB	Age /Ma	Seismic horizon
Erathem era	System period	Series epoch					
Cenozoic	Quaternary	Pleistocene		Ledong Fm.	Wanshan Fm.	1.9	T20
		Pliocene		Yinggehai Fm.	Aohai Fm.	5.5	T30
	Neogene	Miocene	upper	Huangliu Fm.	Hanjiang Fm.	11.6	T40
			middle	Meishan Fm.	Zhujiang Fm.	13.8	T41
			lower	Sanya Fm.	Zhuhai Fm.	15.5	T50
		Oligocene	upper	Lingshui Fm.	Enping Fm.	23.3	T60
			lower	Yacheng Fm.	Wenchang Fm.	29.3	T70
	Paleogene	Eocene		Lingtou Fm.	Shenhu Fm.	32.0	T80
	pre-Cenozoic	–		–	–	53.5	Tg

Note: – represents no data.

into surface circulation (less than 350 m water depth), intermediate water circulation (350–1 350 m), and deep water circulation (more than 1 350 m) (Chen and Wang, 1998). This water core division scheme is widely accepted for bottom currents interpretation, but it is still controversial, especially in the intermediate water depth of division. Newly acquired data indicate that the main scope of the intermediate water can easily exceed a water depth deeper than 1 500 m (Chen et al., 2013; 2016). In the northern QDNB, the unidirectionally migrating canyons, resulted from the interaction between gravity flows and bottom currents, and influenced by northeastward flow bottom currents, were widely developed in water depth from 450 m to 1 500 m. (He et al., 2013). Honeycomb shaped drifts, associated with bottom currents flowing across undulate seafloor, are reported and developed since the early late Miocene (11.6 Ma) in the southwestern QDNB (Sun et al., 2017). Elongated and mounded drifts, resulting from bot-

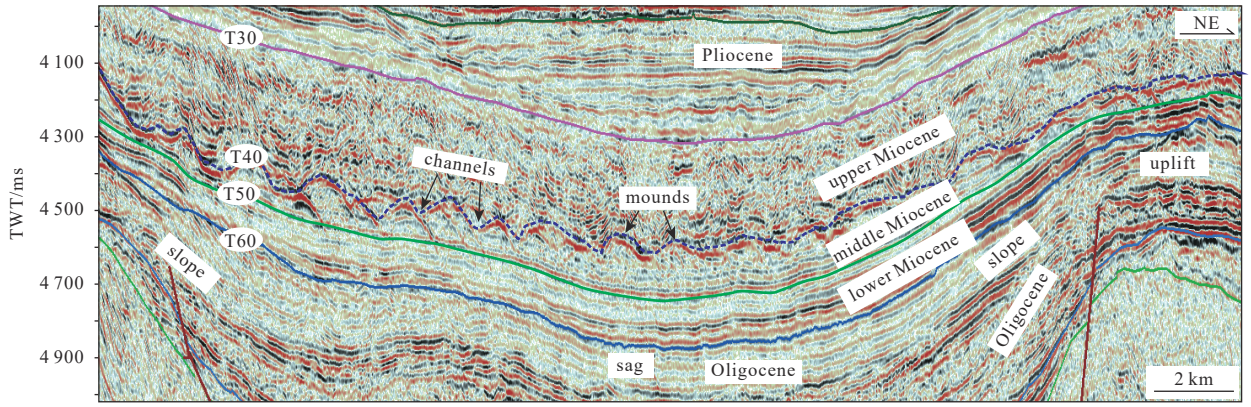

Fig. 3. Characteristics of the mounds at the top of the middle Miocene in the Liwan Sag, ZRMB. The mounds are distributed on the slope and central sag. The bottom of channels between mounds exhibits relatively high amplitudes. The profile location is shown in Fig. 2. TWT: two-way-travel time.

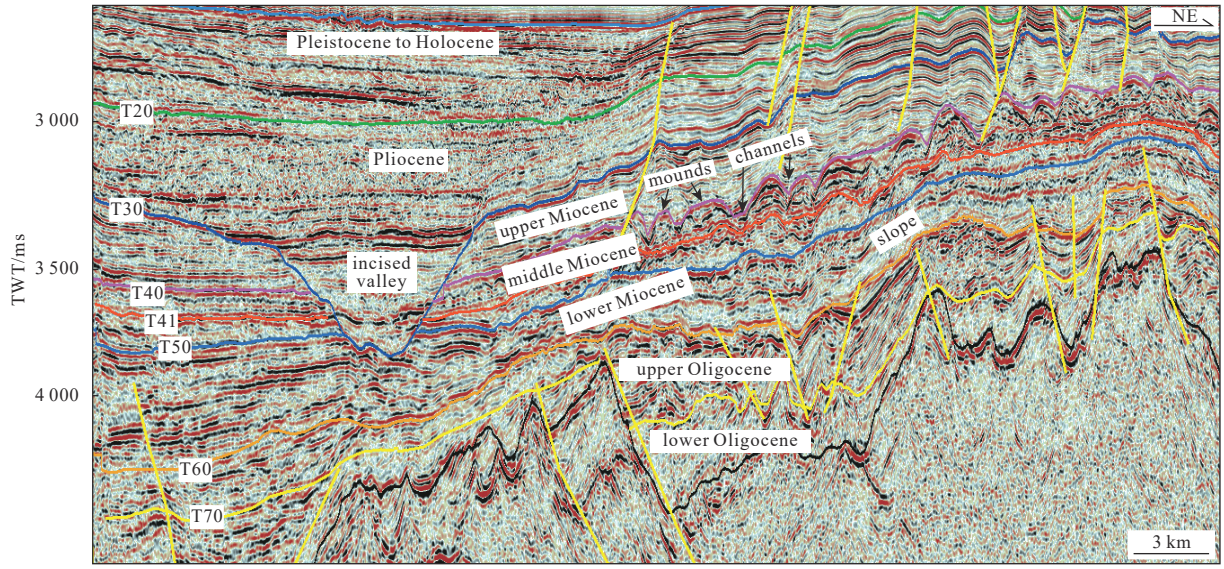

Fig. 4. The middle Miocene mounds are distributed in the slope of the Beijiao Sag, QDNB. The profile location is shown in Fig. 2.

tom currents and related to seamount, can be at least traced back to the early late Miocene (11.6 Ma) in the western ZRMB (Chen et al., 2014). The flow direction of the above-mentioned bottom currents in the ZRMB-QDNB moves from southwest to northeast. It is intimately associated with the intermediate water, which seems to indicate that the bottom currents in the study areas are also associated with the intermediate water. According to present ocean circulation, bottom current deposits are divided into mid-water bottom current deposits (300 m and 2 000 m) and deep-water bottom current deposits (more than 2 000 m) (Stow et al., 2002). Based on these divided schemes, bathyal deposits (current water depth: 600–2 000 m) may be subjected to the influence of the intermediate water in the study areas.

3 Data and methods

Corehole data of multi-oil and multi-gas exploration wells and 2D/3D seismic data are provided by China National Offshore Oil Corporation (CNOOC). The Liwan 3D seismic survey is approximately 1 000 km^2, and the Beijiao 3D survey is approximately 2 000 km^2. Line and trace spacings are 25 m and 12.5 m, respectively, and their sample intervals are 4 ms. Two 3D seismic volumes have a dominant frequency of 40 Hz in the intervals of the target (the middle Miocene interval). The 2D seismic profiles have a vertical seismic resolution of approximately 15 m in the target intervals, with a dominant frequency of approximately 35 Hz. The 2D seismic profile is tied with a drilling well (YLx) with log data to make layers division that is available for an analysis of the lithology of mounds in the Beijiao Sag. Drilling wells from X1, X2, X3, X4, X5, and YLx and the thickness of target layers are utilized to infer sedimentary face of the ZRMB-QDNB in the middle Miocene. Seismic-well tie verifies the age of key seismic reflection horizons. Based on an integrated analysis for the geometry characteristics, paleotectonics, paleogeographic background, and value of seismic impedance inversion within the mound reflections, this study discusses and infers the origin of the channels and mounds in detail.

4 Distribution and geometrical characteristics of the mounds and channels

Currently, the Miocene channels and mounds reflections seen on the seismic profiles in the deep-water area in the ZRMB-QDNB are mainly located in the Liwan Sag and Beijiao Sag. Both

the sags, from one to the other approximately 500 km distance, are nearby the Southern Uplift far away from the shore. The channels and mounds within the sags are mainly distributed from depression centres to/or slopes (Figs 3 and 4). The channels and mounds extend parallelly in the east–west direction (Figs 5a and 6c). The seismic horizons and absolute ages of the channel-mound reflections in the Liwan and Beijiao sags are shown in Table 1. They have the following commonalities or similarities:

(1) In plan view, they are all developed at the top of the

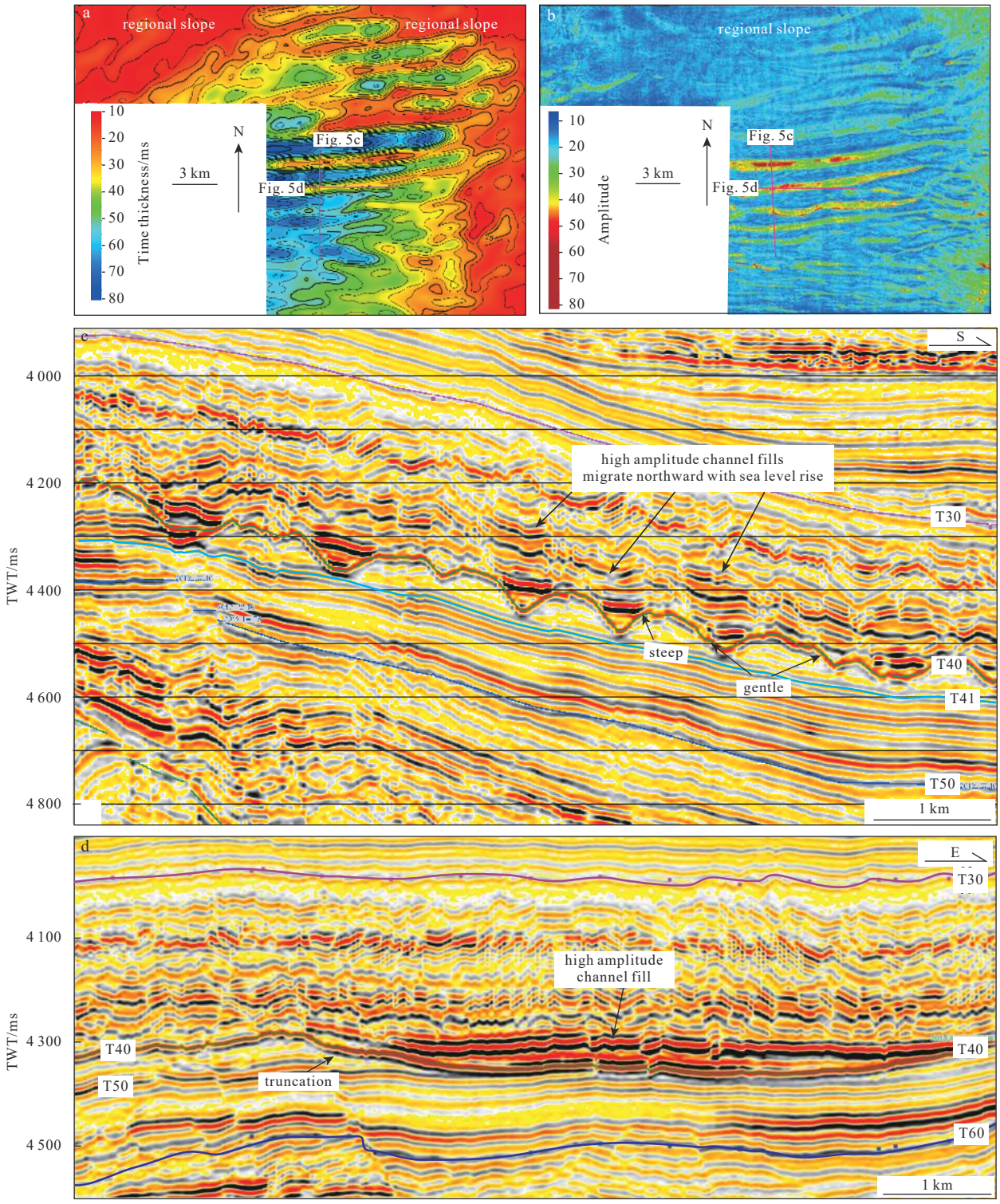

Fig. 5. The characteristics of Miocene channels and mounds in the 3D seismic survey in the Liwan Sag, ZRMB. a. The isochronous map of the remnant mounds (T40–T41); b. the mean-square-root (RMS) amplitude map of time window from the channel bottom T40 to 30 ms upward; c. a north-south 3D seismic profile perpendicular to the channels; d. a near east-west seismic profile along the channels.

middle Miocene in the deep-water area in the southern ZRMB-QDNB and distributed in/at the slopes or sags rather than uplifts (Figs 3 and 4).

(2) The channel bottoms or mound tops are typically erosional unconformities, corresponding to the T40 seismic horizon of approximately 11.6 Ma at the top of the middle Miocene (Table 1). The bottom surface of the remnant mounds is corresponding to horizon T41. The period of the entire mounds in these sags is approximately in the late middle Miocene, while the period of the fills within channels between mounds is in the early late Miocene (Table 1, Figs 3 and 4).

(3) The channels and mounds in the Liwan and Beijiao sags all extend linearly and are arranged parallelly along a near east-west direction. The channel fills show high-amplitude reflections due to the high wave impedance difference of the filling sandstone from mudstone in the Liwan and southwestern Beijiao sags (Figs 5c and 6e).

Apart from the above similarities between channels and mounds in the Liwan and Beijiao sags, their differences are mainly in the below aspects of magnitude, extension direction,

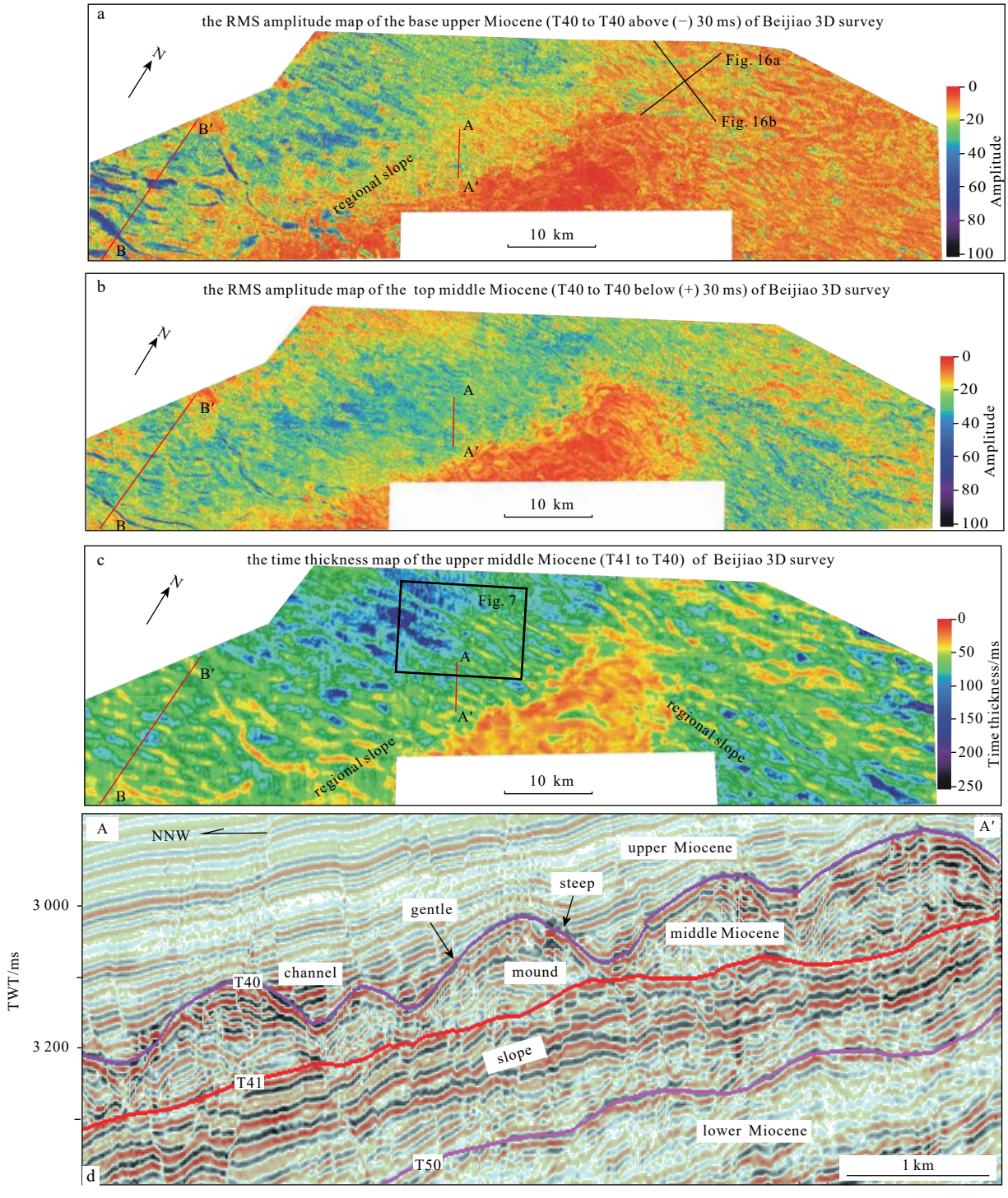

Fig. 6.

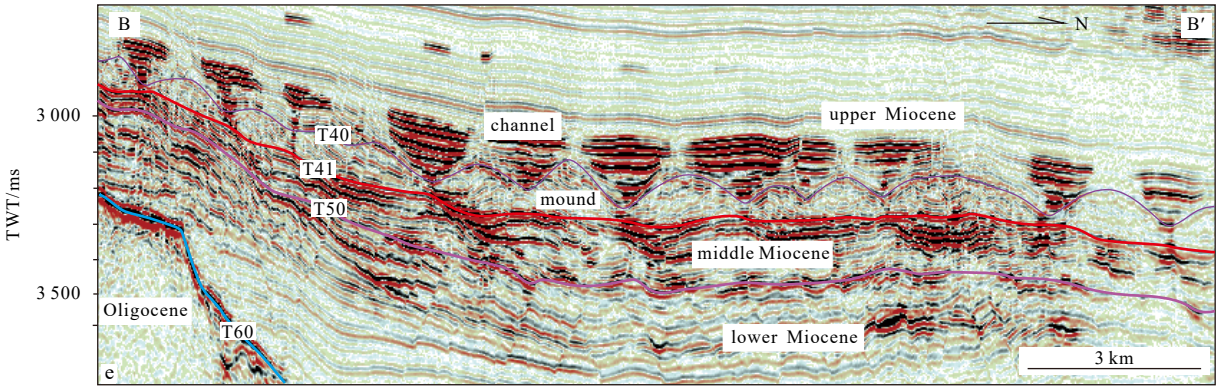

Fig. 6. The characteristics of RMS amplitude maps for channels (a) and mounds (b), the time thickness map (c) and profile of mounds (d, e) in the Beijiao 3D seismic survey. The amplitude of upper Miocene channels is high to mediate-low from the southwestern to northeastern Qiongdongnan Basin, respectively; the mounds between channels are characterized by low amplitudes.

vertical migration, and reflection configuration.

(1) Magnitude differences: the channels and mounds in the Liwan Sag are smaller than those in the Beijiao Sag. The inter-mound distances and mound heights in the Liwan Sag are approximately 1 km and 50–75 ms (100–150 m), respectively (Figs 3 and 5, based on the velocity acoustic wave of Well X3). However, the inter-mound distances and mound heights in the Beijiao Sag are generally 1.5–2.0 km and 100–150 ms (150–200 m), respectively (Figs 4 and 6, based on the velocity acoustic wave of Well YLx).

(2) Differences in amplitude and extension direction: the channels and mounds in the Liwan Sag, parallel to one another, extend linearly in the east-west direction and are parallel with the regional slope (Fig. 5a), exhibiting high and low amplitudes, respectively (Fig. 5c). Mounds in the Beijiao Sag dominantly exhibit relatively low-medium amplitude (Figs 6b, d and e). The channels are characterised by high amplitudes (Figs 6a, d and e) and extend in the northeast-east direction in the west part of the 3D area (Fig. 6c), and they change to moderate amplitudes and extend linearly in a near east–west direction in the middle part (Figs 6d and 7). They locally exterminate on the ancient Beijiao Uplift and are at a small angle to, not parallel with, the regional slope. In the east part, they exhibit relatively low amplitudes and appear to bifurcate (Fig. 6c).

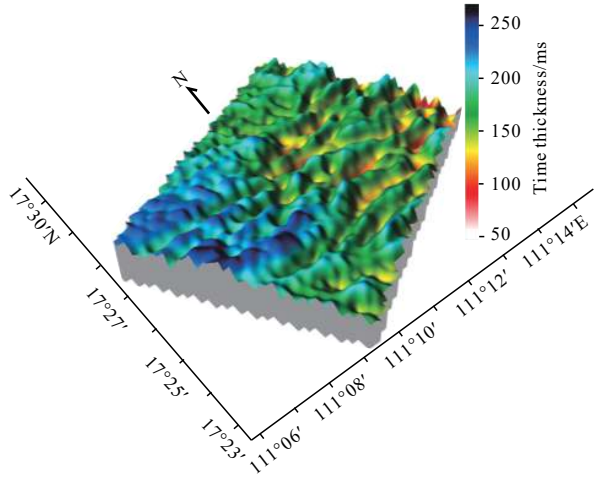

Fig. 7. Time thickness map at the centre of the Beijiao Sag (T40–T41), showing the middle Miocene mounded reflections extending in a near east-west direction as parallel lines. See Fig. 6c for the location.

(3) Differences in the persisting time and migration directions of channels: the channels in the Liwan Sag are only developed in the upper Miocene above horizon T40. The accumulative thickness of the high-amplitude possibly reflecting channel sandstone is approximately 100 ms. The channel locations gradually migrate towards the north from old to young (Fig. 5c). However, the high-amplitude reflections formed by the channels in the Beijiao Sag are developed both in the upper Miocene and in the middle Miocene (Fig. 6e). The accumulative thickness of the high-amplitude reflections is approximately 300 ms. The locations migrate towards the ancient uplift from old to young between T50 and T40, but keep unchanged above T40. Furthermore, the channels below T41 do not cut down to form remnant mounds. The channels in the upper Miocene, however, have vertical aggradations and do not unidirectionally migrate (Fig. 6e).

(4) Differences in the mounded reflection configurations: the internal mounds in the Liwan Sag have the sole type and exhibit low-amplitude parallel reflections (mound type I), parallel with underlying strata (Fig. 5c). Flanks of mounds are characterized by truncation terminations (Fig. 5c). The internal reflection configurations of the mounds in the Beijiao Sag, however, are divided into three types as follows: low-amplitude parallel reflections (mound type I, the same in Liwan Sag), blank or chaotic reflections (mound type II), and internal mounded reflections (mound type III) (Fig. 8). There is not an obvious discipline about the distribution of three types of mounds in the Beijiao Sag.

5 Paleotectonic and paleogeographic setting of the mounds and channels

Through the thickness map of the middle Miocene (T50–T40) in the southern deep-water area of the ZRMB-QDNB, it shows the paleotectonic setting of the development period of the mounds and channels. Similar to the uplift and depression configuration shown in Fig. 2, the Liwan Sag and Beijiao Sag are in the depression region to the north part of the Southern Uplift in the ZRMB-QDNB during middle Miocene deposition stage. The middle Miocene strata thicknesses of Liwan Sag and Beijiao Sag range from 250 m to 400 m and from 150 m to 250 m, respectively (Fig. 9). The thickness of the uplift is 0–150 m. The Southern Uplift may experience local erosion or sedimentary hiatus. This tectonic appearance is still characterized by a transitional basin type from a depression basin to a continental-margin basin.

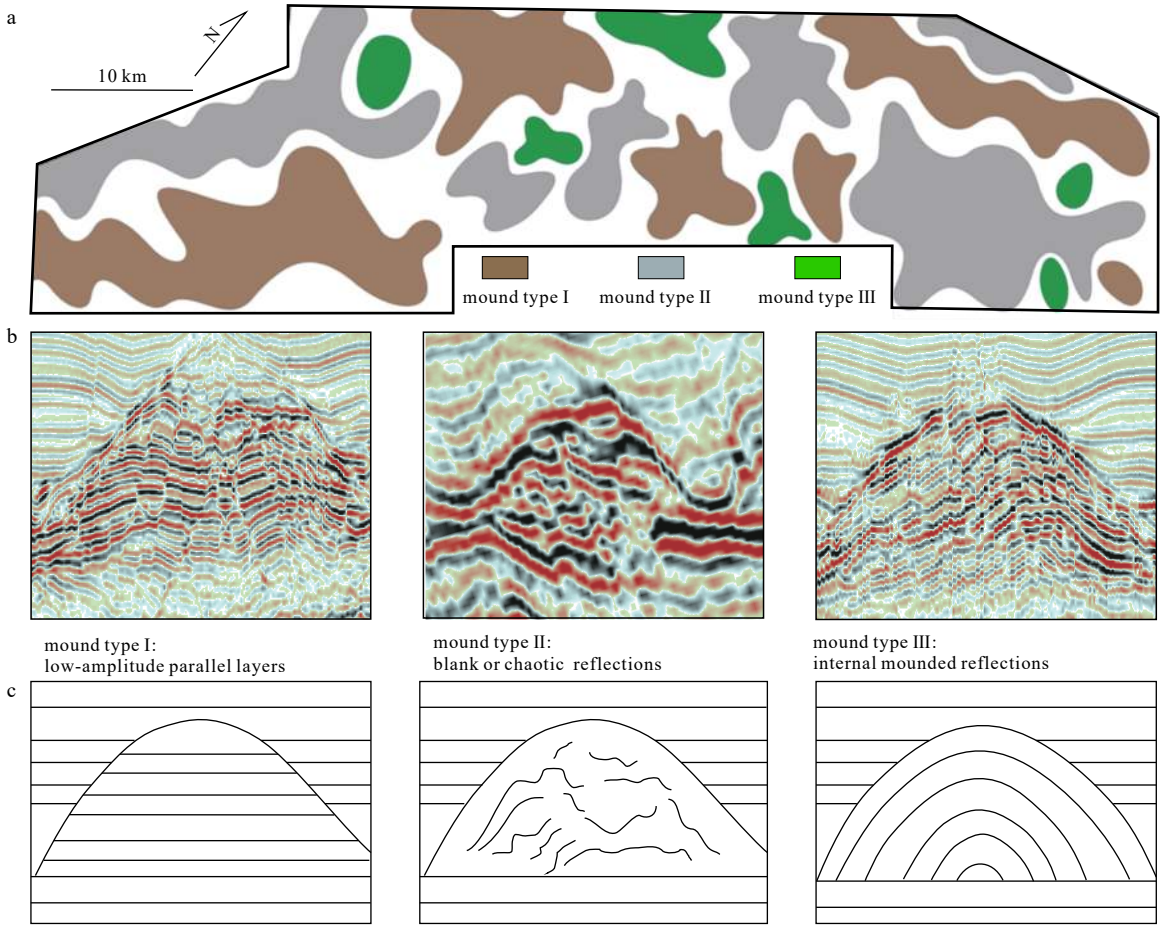

Fig. 8. Horizontal distribution (a) and three types (b and c) of internal structures of mound reflections in the Beijiao Sag. Polygonal faults are developed within the mounds (Li et al., 2017a), to some extent, which disturb the discipline of the three types mounds and make seismic reflections within mounds unclear.

Drilling wells confirm that carbonate platforms occur on some ancient uplifts since the early Miocene in the northern SCS (Shao et al., 2017). In the area adjacent to Liwan Sag, Well X5 also verifies the carbonate platform is developed in the early Miocene (Fig. 10), which consists of domolite. X2, X3 and X4, however, dominantly consist of siltstone, marlstone, and sandstone, which would be deposited in the neritic environment. The Well X1 mainly consists of tuff and may be also deposited in the same environment in the early Miocene. However, due to the rapid relative sea level rise in the middle Miocene (Zhang, 2010), X2, X3, X4 and X5 mainly consist of mudstone locally interbedded with thin siltstone, and they are all developed in the bathyal environment. X1 mainly contains siltstone, obviously contrasting with the other wells, and may be persistently developed in the neritic environment.

Synthesizing analysis on the multiple wells in the shallow to deep water areas, the insight into basin structure, and strata thickness variation from 2D and 3D seismic data in the deep-water area, a sedimentary facies map of the ZRMB-QDNB in the middle Miocene is produced (Fig. 11). In the middle Miocene, delta or gravity flow sandstones are mainly deposited in the northern part of ZRMB-QDNB. Bathyal faces are distributed in the middle part and are composed of mudstone interbedded silts and calcareous mudstones (Fig. 10). Excluding the above areas, neritic face is widely distributed in the ZRMB-QDNB. Carbonate platform and carbonate clinoform (Fig. 11) are mainly developed in the topographical high, i.e., relatively thin isopach area (Fig. 9). In the middle Miocene, Beijiao and Liwan sags are located in the bathyal environment, indicating that the mounds and channels are developed in a deep-water environment. Since the middle Miocene, these two regions (Liwan and Beijiao) are mainly composed of abyssal mudstone deposits. The water depth gradually increases upward, corresponding to broad low-amplitude reflections in the seismic profiles (Figs 3–6).

Currently, only the Well YLx has drilled through the flank of a middle Miocene mound reflection in the Beijiao Sag. The corresponding strata lithologies are composed of mudstone interlayered with calcareous mudstone in the Meishan Formation (Fig. 12).

6 Analysis on wave-impedance characteristics of the mounds

Wave impedance profiles (Figs 13 and 14) for the mounds were obtained using the sparse pulse inversion method. The average value of the wave impedance inside the mounds is less than 6.5×10^6 kg/(m^2·s) (Fig. 13) in the ZRMB. Counterpart inside the mounds is less than 6.0×10^6 kg/(m^2·s) (Fig. 14) in the QDNB. In the northern SCS, the average value of the wave impedance for reef varies from 8 kg/(m^2·s) to 12×10^6 kg/(m^2·s) (Wu et al., 2009; Tian et al., 2015). The counterpart for compact limestone is much more than 10×10^6 kg/(m^2·s) (Tian et al., 2015). The counterpart between sandstone and mudstone changes from 6×10^6 kg/(m^2·s) to 8×10^6 kg/(m^2·s) (Tian et al., 2015). As discussed above, these

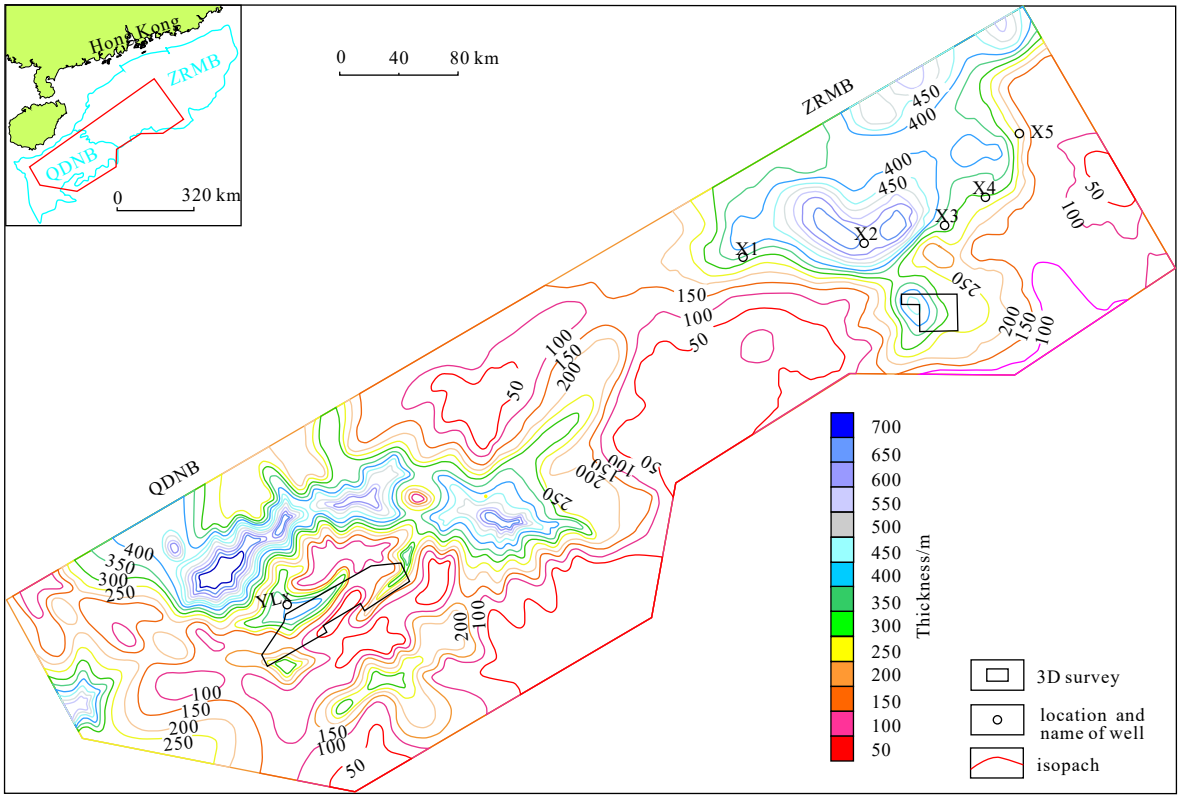

Fig. 9. Isopach map of the ZRMB-QDNB (T50–T40), indicating that both Beijiao Sag and Liwan Sag with channels and mounds reflections are located in the tectonic depression with relatively thick sediments.

results suggest that the mounds from Liwan and Beijiao sags mainly consist of mudstone rather than limestone/dolostone, which is in accordance with the drilling Well YLx (Fig. 12).

7 Paleo-bottom current flow direction

According to the lee wave model, the migration direction of crests and troughs of bottom-current sediment waves corresponds to the upstream flow direction of bottom currents (Flood and Giosan, 2002). Above the middle Miocene mounds, the widespread distributions of bottom-current sediment waves are documented in previous studies in the Beijiao area (Zhao et al., 2013; Tian et al., 2015). The crests and troughs of bottom-current sediment waves have migrated southwestward since the late Miocene (Fig. 15), which indicates that bottom currents have flowed northeastward since the early late Miocene and seems to imply that the bottom currents are associated with the intermediate water. The inner mounds are characterised by blank or chaotic seismic reflection, which seems to be turbidite. The phenomenon will be further discussed in the following text in detail.

8 Discussion

8.1 *Distribution and shape characteristics of the mounds*

Reefs are generally characterized by special shapes such as a patch shape, a pinnacle shape, and an atoll shape (Wilson, 1975). Mud diapers and mud volcanoes are often observed as isolated and/or irregular distribution and chaotic seismic reflections, occasionally single channel-shaped distribution (Chen et al., 2015). In the Liwan and Beijiao sags, however, the mounds and channels are parallel to each other, linear and spaced array, large-scaled distribution (Figs 5a and 6c), and sinusoidal shape (Figs 3, 4, 5c and 6d), which obviously differ from the distribution characteristics of reefs, mud diapers and mud volcanoes. Consequently, it seems to indicate the mounds would not be the origins of reefs, mud diapers and mud volcanoes.

8.2 *Paleo-tectonic setting and sedimentary environment*

In 3D study surveys, all the mounds and channels are located in the Liwan and Beijiao sags rather than uplifts. Reefs, however, are difficultly survived/developed in these sags. Reefs generally occur in the topographic high such as platform and uplift. Through an integrated analysis of the seismic attribute, palaeotectonics, palaeogeography, thickness of middle Miocene (T50–T40), and drilling well data, research results show Liwan and Beijiao 3D study surveys are located in the bathyal environment (Fig. 11), consistent with previous studies (Zhao et al., 2013; Tian et al., 2015; Sun et al., 2016; Liu et al., 2016; Li et al., 2017b, 2018), where the deepwater environment makes reefs hardly survive. It is well known gentle flanks of reefs towards uplift (shallow-water setting) and steep flanks towards sag/slope (deepwater setting). There are, however, contrasting trends that the gentle flanks of mounds toward the sags and the steep flanks towards the uplifts (Figs 5c and 6d). Consequently, it may be impossible that the mounds are reefs.

8.3 *Wave impedance and seismic amplitude*

The average values of the wave impedance inside mounds in Liwan and Beijiao sags are less than 6.5×10^6 kg/(m^2·s) and 6.0×10^6 kg/(m^2·s), respectively, both of which are lower than those inside reefs and compact limestone (approximately 8×10^6 kg/(m^2·s) and 10×10^6 kg/(m^2·s), respectively). This implies that the mounds would be attributed to the scope of the mud-

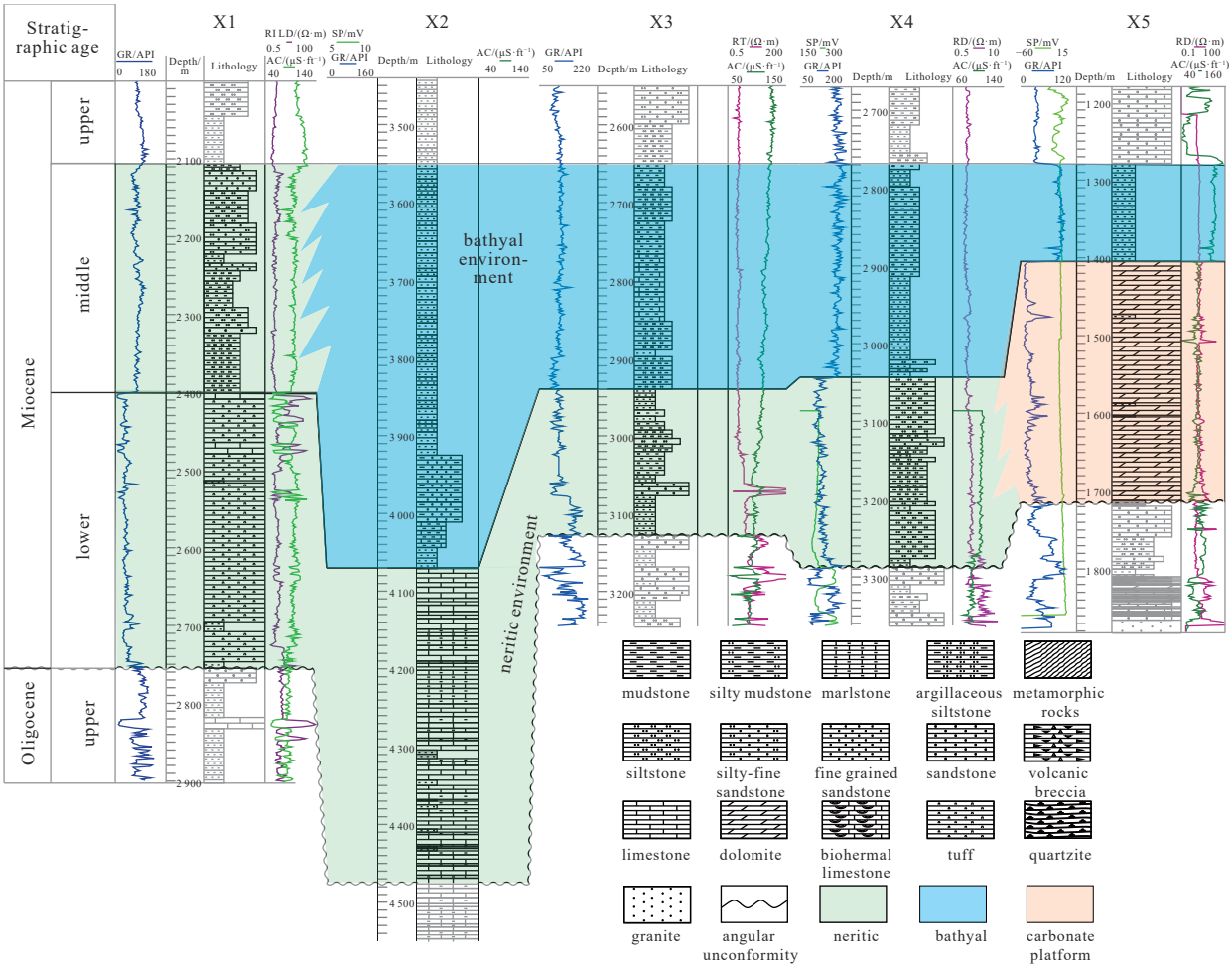

Fig. 10. The comparative section of sedimentary facies for connecting wells of the middle and lower Miocene in the ZRMB. The section location is shown in Figs 2 and 11. GR: natural gamma ray, RILD: resistivity of deep investigate induction log, SP: spontaneous potential, AC: acoustic, RT: true formation resistivity, RD: deep investigate double lateral resistivity log.

stone and/or sandstone. Furthermore, compared to channels filled by high amplitudes (suggested sandstone), the mounds in the Beijiao and Liwan sags are low-mediate amplitudes (indicated mudstone) (Figs 5c and 6e). In addition, drilling Well YLx also verifies the mounds dominantly consist of mudstones. Consequently, these suggest that the mounds are mainly composed of mudstones rather than reefs and limestone.

8.4 *The vigorous bottom currents*

The thermohaline (bottom current) circulation from middle Miocene to Pliocene in the northern South China Sea is relatively stable and vigorous (Zhao, 2013), which is closely related to the regional tectonic evolution in the South China Sea and the strengthening of Kuroshio (Zhu et al., 2010). The formation of Kuroshio is associated with the closure of the most important seaways such as the Tethys, Panama, and Indonesia in the world. The Tethys pathway becomes shallow and closed in the early Miocene (Dercourt et al., 2000). The Panama pathway is approximately 1 000 m deep at 12 Ma (Duque-Caro, 1990), and finally becomes shallow and closed at approximately 3.5 Ma (Keigwin, 1982). The collision between the Australian plate and Eurasian plate, resulting in the closure of the Indonesia pathway, approximately occurred in the early Miocene (Kuhnt et al., 2004) or middle Miocene (Tsuchi, 1997). The Kuroshio circulation in the Pacific is greatly enhanced by this effect (Tsuchi, 1997), which contributed to the vigorous bottom current activities in the South China Sea in the early or middle Miocene. Furthermore, in the northwestern SCS the contourites, mounds and channels related to bottom currents are documented in previous studies (Shao et al., 2007; Gong et al., 2012, 2016; Li et al., 2013, 2017b, 2018; Chen et al., 2016; Tian et al., 2015; Sun et al., 2016, 2017). In the QDNB they can be traced back to the late early Miocene (Sun et al., 2016) or the middle Miocene (Tian et al., 2015; Li et al., 2018). Therefore, it is inferred that the two sags are in the condition for the development of vigorous bottom currents, which provides capacity for incising underlying strata in the early late Miocene.

In the Beijiao Sag, a number of bottom-current sediment waves are developed in the middle and upper Miocene (Zhao et al., 2013; Tian et al., 2015; Li et al., 2018). Mounds and channels incised by bottom currents are documented in previous studies in the Miocene in the Beijiao Sag (Pu et al., 2013; Tian et al., 2015; Li et al., 2017b, 2018). Mounds and channels originated from the downcut of bottom currents are reported in the Liwan Sag (Pu et al., 2013; Sun et al., 2016). Bottom currents, incising or downcutting the underlying strata to form the remnant mounds and channels, are reported in previous studies in the

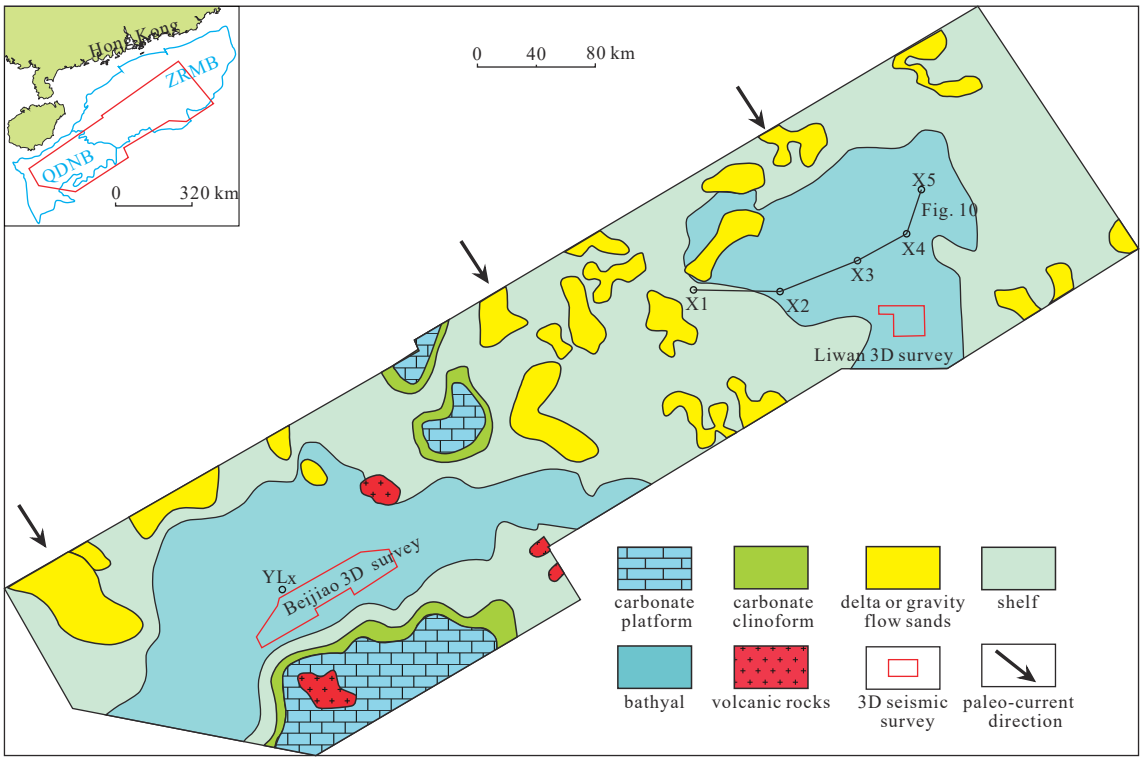

Fig. 11. Middle Miocene (T50–T40) sedimentary facies map of the ZRMB and QDNB, indicating that the channels and mounds are developed in the bathyal environment.

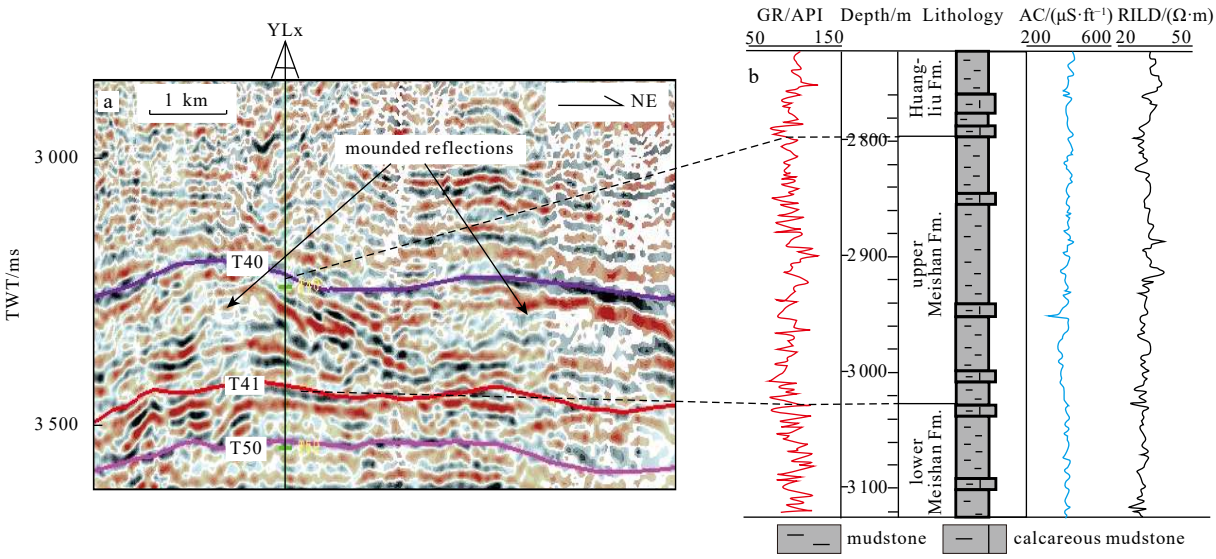

Fig. 12. Well YLx logging and lithology profiles corresponding to the mound reflections in the Meishan Fm. in the Beijiao Sag of the Qiongdongnan Basin. Fm.: represents formation.

SCS (Sun et al., 2016; Li et al., 2017b). Remnant mounds and channels, originated from the incision of bottom currents, are also documented in other studies in the North Sea (Stuart and Huuse, 2012). The characteristics of mounds (type I) and channels in the Liwan and Beijiao sags are similar with them, which seems to indicate they have the same origin.

Continuous parallel-layered seismic reflections inside mounds in the northeastern Beijiao Sag are parallel with underlying strata, which exhibit low-moderate amplitudes and truncations at the flanks of mounds (Fig. 16). Furthermore, channel filled between mounds are characterized by low amplitudes obviously contrasting to the high amplitudes filled in channels in the Liwan Sag (Figs 5c and d) and southwestern Beijiao Sag (Fig. 6e), showing onlaps on the sides of channels. Moreover, the channels are in the low mean-squre-root area (Fig. 6a). These features indicate gravity flows do not occur or downcut the underlying strata within channels in the northeastern Beijiao Sag. The origin for the channels with low-medium amplitudes would be the early (initial) incision and late deposit of bottom currents. Mounds (type I) are remnant underlying strata incised by bot-

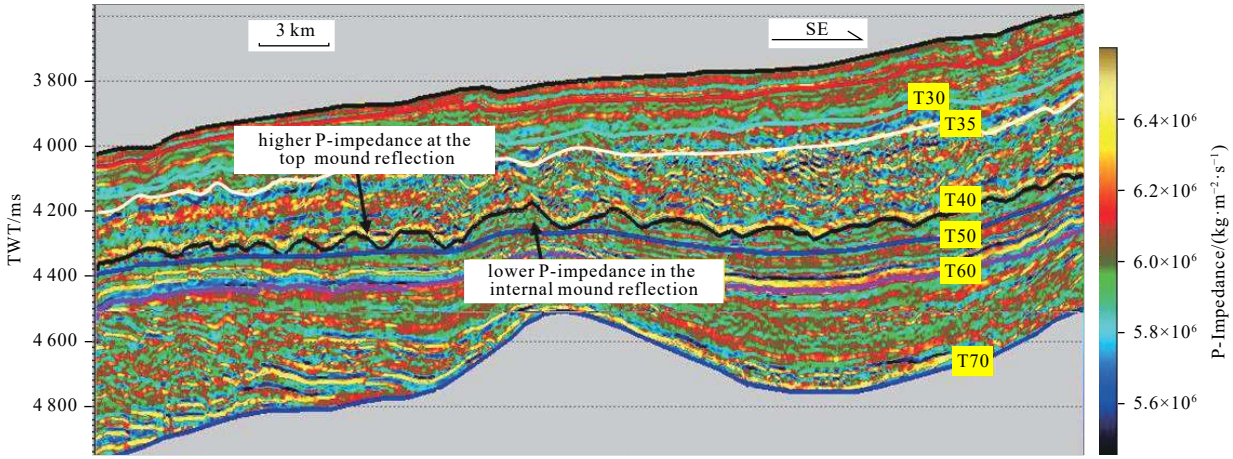

Fig. 13. The wave impedance profile for the Liwan Sag. The average value for the wave impedance of mounds is less than 6.5×10^6 kg/(m²·s). Location is shown in Fig. 2.

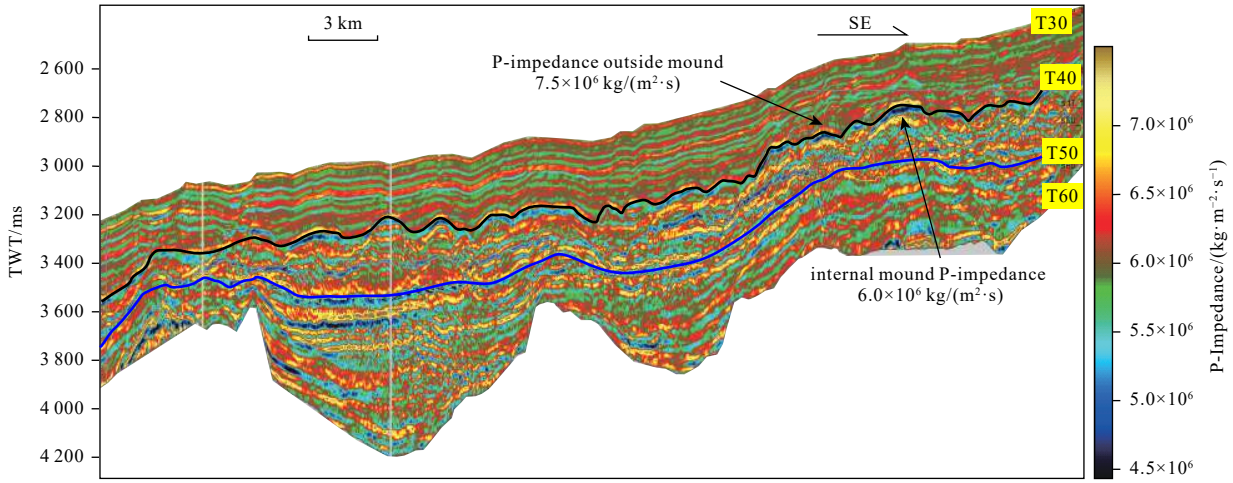

Fig. 14. The wave impedance profile for the Beijiao Sag. The average value for the wave impedance of mounds is less than 6.0×10^6 kg/(m²·s). Location is shown in Fig. 2.

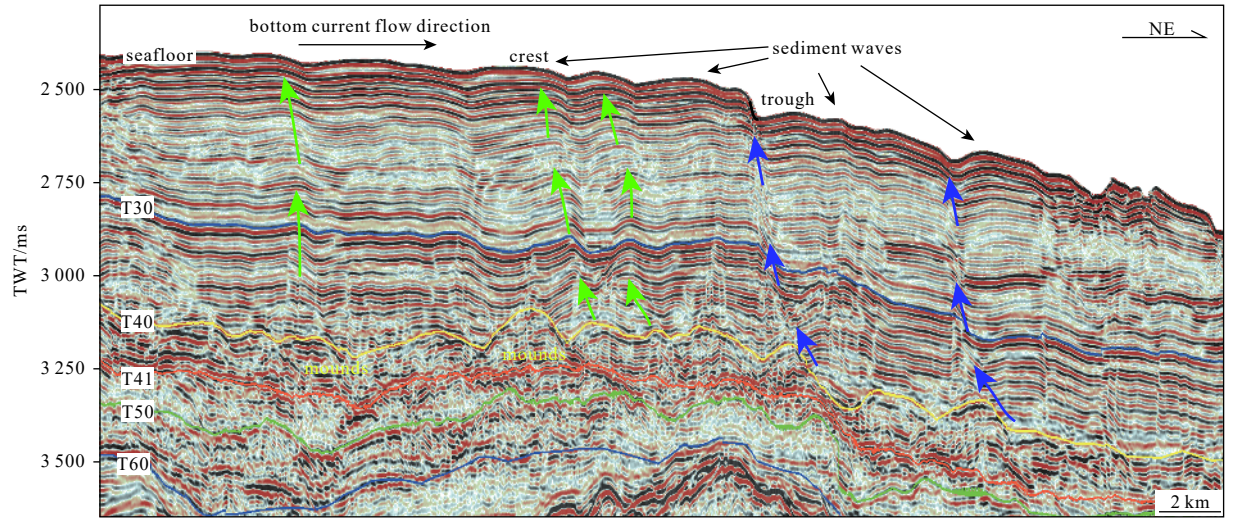

Fig. 15. The migration characteristics of bottom-current sediment waves. It shows crests and troughs of sediment waves have migrated southwestward since the early late Miocene, which suggests that bottom currents persistently move northeastwards in the early late Miocene. Green and blue solid arrows represent unidirectional migration of crests and troughs of sediment waves, respectively. See location in Fig. 2.

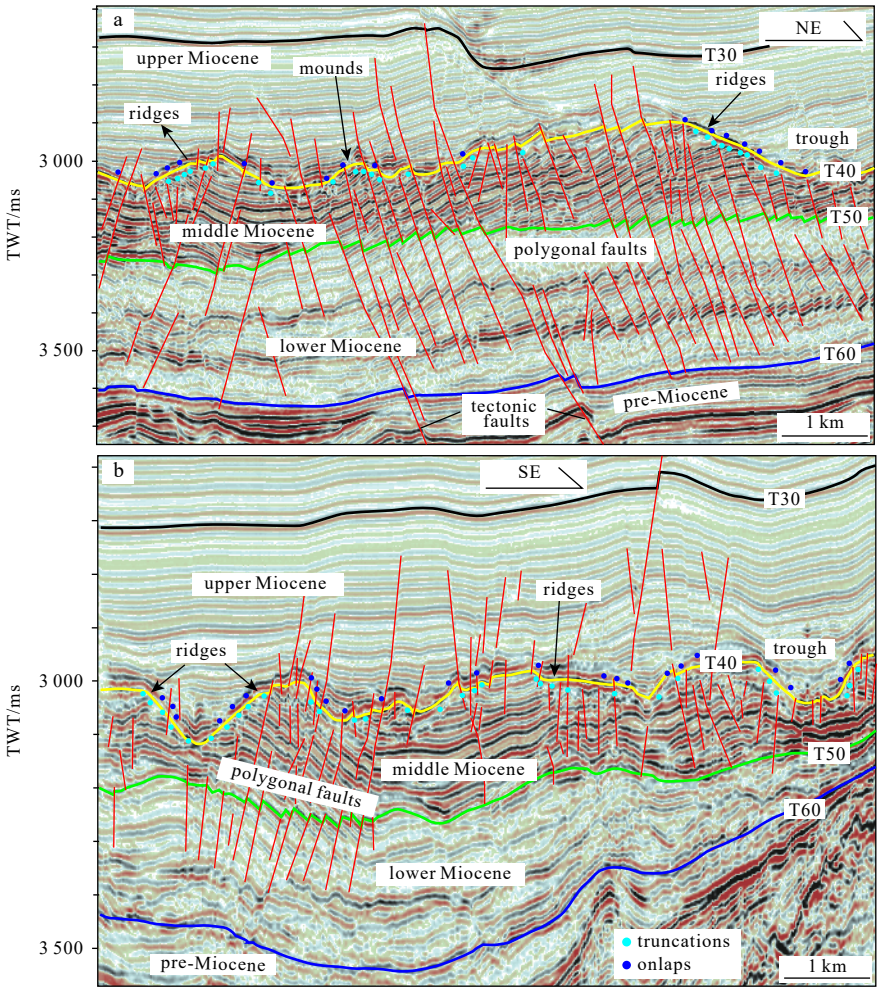

Fig. 16. Seismic profile showing seismic contact characteristics among mounds, channels and polygonal faults. Blue and dark blue dots stand for truncations and onlaps, respectively. See locations in Fig. 6a.

tom currents. Polygonal faults are widely developed within mounds (Fig. 16) and attributed their origins to gravity spreading and overpressure syneresis (Li et al., 2017a). Polygonal faults are mainly developed in the fine-grained sediments in the deep water environment (such as mudstone), northern SCS (Li et al., 2017a), where bottom currents can be prone to occur. Hitherto, polygonal faults within reef mounds have not been documented in literature, suggesting mounds less likely result from reefs.

8.5 *Submarine landslide*

Submarine landslide is mainly classified into the slide, creep, spread, debris flows and turbidity flows (Masson et al., 2006). They are the main gravity-driven processes during which marine sediments are transported downslope (Masson et al., 2006). Generally speaking, the steeper the slope is, the higher the probability of landslide is. Regional slopes are developed in the two sags adjacent to Southern Uplift (Figs 3 and 4).

Since the early Miocene subsidence rate of QDNB is higher than that of Southern Uplift (Wu et al., 2014), indicating the southern paleoslope where the Beijiao Sag is located may become steeper. Moreover, amounts of carbonate were widespreadly developed on the Southern Uplift in the middle Miocene (Fig. 11). In these cases, Southern Uplift might provide provenance (such as carbonate) for submarine landslide and sediments transported downslope. Landslide phenomenon is found within mounds, such as gravity spreading (Li et al., 2017a), creep, and turbidity flows (Tian et al., 2015). This is the possible reason why mounds contain a few calcareous mudstones (Fig. 12). Creep of sediments is prone to generate compressional ridge-like waves (herein mounds) (Tian et al., 2015), the same to slide and spread. Moreover, gravitational spreading within mounds results in polygonal faults in the Beijiao Sag (Li et al., 2017a) (Fig. 16). Turbidites with blank or chaotic reflection (mound type II) are also observed in Fig. 15.

Thereafter, the initial compressional ridge-like waves are incised and reshaped by bottom currents into current shapes/topographies of channels and mounds, corresponding to the truncations at the flanks of mounds. As the weakening of bottom currents, fine-grained sediments are deposited within channels and characterized by low amplitude in the upper Miocene (Fig. 16). Bottom-current sediments waves over the mounds and channels persistently migrate northwestward (Fig. 15). The Beijiao Sag is in a period of low sea level (lowstand system tract) and then prone to trigger gravity (turbidity) flows from Southern Uplift in the early late Miocene. Turbidity flows occur in the southwestern part of the Beijiao 3D study area (Figs 6a and e) and are steered by early channels and mounds. They incise underlying strata and make the mounds and channels bigger. With the slope gradient

reduction and weakening of gravity flows, they are deposited within channels exhibiting high amplitudes (Figs 6a and e), i.e., channels with high amplitudes are filled by sandstones from deposits of turbidity flows.

Delta or gravity flow sands are developed around Liwan Sag in the middle Miocene (Fig. 11), suggesting large amounts of gravity-flow provenance. The Liwan Sag was also in a period of low sea level (lowstand system tract) and then prone to trigger gravity flow in the early late Miocene. Erosional troughs (herein early channels) are documented and result from the incision of bottom currents (Sun et al., 2016). Later, gravity flows from Southern Uplift are steered by the early (initial) channels and incise the underlying strata to form remnant mounds and channels along the strike of the regional slope. Therefore, it is inferred that high-amplitude channels (Figs 5b–d) consist of sandstones from gravity flows. This is why both mounds and channels in Beijiao and Liwan sags extend linearly and are parallel to one another.

8.6 *The seismic reflection characteristics and origins of mounds*

The internal mounds in the Liwan Sag are characterized by the subparallel/parallel seismic reflection configuration (mound type I) (Fig. 5c). They are parallel with the underlying strata. Three mound types occur in the internal mounds in the Beijiao Sag (Fig. 8). The mound type I in the Liwan and Beijiao sags have the same seismic reflections, which implies they possibly have the same origin, i.e., incision of bottom currents or/and gravity flows. This result, to some degree, corresponds with remnant mounds originated from the incision of bottom currents (Li et al., 2017b), the combination of bottom currents and turbidity flows (Tian et al., 2015) in the Beijiao Sag. Previous literature has documented that there is a giant channel, 30 km wide and 50 km long, with high amplitude (suggested by sandstone) in the eastern Liwan Sag (Liao et al., 2016) and that gullies (herein channels between mounds) and sediment waves originated from turbidity flows are widely developed in the Liwan Sag (Liu et al., 2016). Consequently, it is inferred that channels between mounds are filled by high amplitude (sandstone originated from turbidite flows) in the Liwan Sag and southwestern Beijiao Sag. Other channels, however, are filled by low-medium amplitude (mudstone) in the middle and northwestern Beijiao Sag.

The mound type II may result from gravity-driven sediments such as turbidite (Figs 8 and 15), which can form blank or chaotic seismic reflection. Gravity flows are reported and developed in the Beijiao Sag in the upper middle Miocene (Tian et al., 2015). There are also widespread turbidity sediment waves in the vicinity of central channels in the middle QDNB (Jiang et al., 2013), which may suggest that waves or mounds (chaotic reflection) in Fig. 8 are originated from turbidity (gravity) flows. Since the early Miocene subsidence rate of QDNB are higher than that of Southern Uplift (Wu et al., 2014), indicating the paleoslope might become steeper. Under the influence of gravity, sediments are prone to slide and form sliding folds exhibiting mounded shape in the regional slope (Bull et al., 2009). The study area adjacent to Southern Uplift is located in the regional slope and it has the capacity to slide and result in mounds (sliding compressional folds) such as Fig. 15. Meanwhile, this type may also be multiple wave artifacts caused by the large wave impedance difference at the mound top surface, particularly in 2D seismic profile, which needs to be discussed further in future.

The mound type III seems to be a product of deposition and incision of bottom currents simultaneously. It may be not of remnant-mound origin but more likely of sedimentary-mound origin; i.e., the channel incision and mound deposition occur simultaneously. These mounds are characterized by high amplitude at the top of mounds and low-mediate amplitude at the bottom of mounds, which differ from the reefs with high amplitudes at the top and bottom. These features are also different from the mud diapir, paleopockmarks, sediment waves and sedimentary deformation. A number of sediment waves associated with bottom (contour) currents are oriented at an angle to both the current direction and (regional) slope (Gong et al., 2012; Hernández-Molina et al., 2017). According to the lee wave (bottom-current sediment waves) (Flood, 1988), when bottom currents flow across mounds (waves), they generate high sedimentation rate on the upstream side of mounds and erosion/low sedimentation rate on the downstream side, i.e., simultaneous deposition and incision of bottom currents. In this case, these may be why the mounds are asymmetry, one side gentle and the other steep (Fig. 6d). The asymmetry of mounds is also documented (Tian et al., 2015). Consequently, the mounds are possibly bottom-current sediment waves, which are consistent with mounds originated from bottom-current sediment waves in the Beijiao Sag (Zhao et al., 2013).

However, these three types are nearby on the plane and slightly extend in the northeast-east direction (Fig. 8). The distribution locations, sizes, and numbers of these mounds do not strictly correspond with mounds in Fig. 6b, which may imply their other complex origins that need to be further researched in future.

9 Conclusions

Channels and mounds are widely developed at the top of the middle Miocene in the Liwan and Beijiao sags far away from the shore in the northern South China Sea. Almost all of the channels and mounds extend linearly in a near east-west direction. They are at a small angle to the strike of the slope in Beijiao Sag and parallel with the strike of the regional slope in Liwan Sag. Both mounds and channels occur on the depression centres and/or slopes rather than uplifts, and mainly exhibit spacing distribution at intervals. Based on the integrated analysis on the wave impedance inversion, drilling well data, distribution and geomorphology of mounds, reflection characteristics of inner mounds and polygonal faults, the mounds and channels are inferred to be formed and developed in the bathyal sedimentary environment.

Three type mounds (types I–III) are distributed in the Beijiao Sag, however, only one (type I) in the Liwan Sag. The mounds (type I), characterised by the subparallel/parallel seismic reflection configuration in the Beijiao and Liwan sags, originate from the incision of bottom currents and/or gravity flows in the early late Miocene. The mounds (type II) with blank or chaotic seismic reflection may result from gravity-driven sediments such as turbidites. The mounds (type III) with internal mounded reflections are the product of deposition and incision of bottom currents, simultaneously.

Channels with high amplitudes are a result of gravity-flow sediments and suggest sandstones in the Beijiao and Liwan sags, whereas channels with low-mediate amplitude originate from bottom-current sediments and are dominantly composed of mudstones in the Beijiao Sag.

References

Andresen K J, Clausen O R, Huuse M. 2009. A giant (5.3×10^7 m^3) middle Miocene (c. 15 Ma) sediment mound (M1) above the Siri Canyon, Norwegian–Danish Basin: Origin and significance.

Marine and Petroleum Geology, 26(8): 1640–1655, doi: 10.1016/j.marpetgeo.2009.02.005

Bull S, Cartwright J, Huuse M. 2009. A review of kinematic indicators from mass-transport complexes using 3D seismic data. Marine and Petroleum Geology, 26(7): 1132–1151, doi: 10.1016/j.marpetgeo.2008.09.011

Chen C T A, Wang Shulun. 1998. Influence of intermediate water in the western Okinawa Trough by the outflow from the South China Sea. Journal of Geophysical Research, 103(C6): 12683–12688, doi: 10.1029/98JC00366

Chen Hui, Xie Xinong, Van Rooij D, et al. 2013. Depositional characteristics and spatial distribution of deep-water sedimentary systems on the northwestern middle-lower slope of the Northwest Sub-Basin, South China Sea. Marine Geophysical Research, 34(3–4): 239–257, doi: 10.1007/s11001-013-9191-7

Chen Hui, Xie Xinong, Van Rooij D, et al. 2014. Depositional characteristics and processes of alongslope currents related to a seamount on the northwestern margin of the Northwest Sub-Basin, South China Sea. Marine Geology, 355: 36–53, doi: 10.1016/j.margeo.2014.05.008

Chen Hui, Xie Xinong, Zhang Wenyan, et al. 2016. Deep-water sedimentary systems and their relationship with bottom currents at the intersection of Xisha trough and Northwest Sub-Basin, South China Sea. Marine Geology, 378: 101–113, doi: 10.1016/j.margeo.2015.11.002

Chen Jiangxin, Song Haibin, Guan Yongxian, et al. 2015. Morphologies, classification and genesis of pockmarks, mud volcanoes and associated fluid escape features in the northern Zhongjiannan Basin, South China Sea. Deep Sea Research Part Ⅱ: Topical Studies in Oceanography, 122: 106–117, doi: 10.1016/j.dsr2.2015.11.007

Chen Lei, Lu Yongchao, Wang Zhenfeng, et al. 2011. Structure of carbonate platform margin and characteristics of reef and their controlling factors in western deep-water region of South China Sea. Petroleum Geology and Experiment (in Chinese), 33(6): 607–612

Dercourt J, Gaetani M, Vrielynck B, et al. 2000. Atlas Peri-Tethys: Palaeogeographical Maps. Paris, France: Commission for the Geological Map of the World, 268.

Duque-Caro H. 1990. Neogene stratigraphy, paleoceanography and paleobiogeography in Northwest South America and the evolution of the Panama Seaway. Palaeogeography, Palaeoclimatology, Palaeoecology, 77(3–4): 203–234, doi: 10.1016/0031-0182(90)90178-A

Flood R D. 1988. A lee wave model for deep-sea mudwave activity. Deep Sea Research, 35(6): 973–983, doi: 10.1016/0198-0149(88)90071-4

Flood R D, Giosan L. 2002. Migration history of a fine-grained abyssal sediment wave on the Bahama Outer Ridge. Marine Geology, 192(1-3): 259–273, doi: 10.1016/S0025-3227(02)00558-3

Gong Chenglin, Wang Yingmin, Peng Xuechao, et al. 2012. Sediment waves on the South China Sea Slope off southwestern Taiwan: Implications for the intrusion of the Northern Pacific Deep Water into the South China Sea. Marine and Petroleum Geology, 32(1): 95–109, doi: 10.1016/j.marpetgeo.2011.12.005

Gong Chenglin, Wang Yingmin, Zheng Rongcai, et al. 2016. Middle Miocene reworked turbidites in the Baiyun Sag of the Pearl River Mouth Basin, northern South China Sea margin: Flow processes, genesis, and implications. Journal of Asian Earth Sciences, 128: 116–129, doi: 10.1016/j.jseaes.2016.06.025

He Yunlong, Xie Xinong, Kneller B C, et al. 2013. Architecture and controlling factors of canyon fills on the shelf margin in the Qiongdongnan Basin, northern South China Sea. Marine and Petroleum Geology, 41: 264–276, doi: 10.1016/j.marpetgeo.2012.03.002

Hernández-Molina F J, Campbell S, Badalini G, et al. 2017. Large bedforms on contourite terraces: Sedimentary and conceptual implications. Geology, 46(1): 27–30

Huang Hongguang, Lu Yongchao, Zou Zhuochao. 2012. Application of seismic sedimentology in platform edge reef, Songnan 3D area, Qiongdongnan Basin. Petroleum Geology & Experiment (in Chinese), 34(1): 25–29

Jiang Tao, Xie Xinong, Wang Zhenfeng, et al. 2013. Seismic features and origin of sediment waves in the Qiongdongnan Basin, northern South China Sea. Marine Geophysical Research, 34(3-4): 281–294, doi: 10.1007/s11001-013-9198-0

Keigwin L. 1982. Isotopic paleoceanography of the Caribbean and east Pacific: Role of Panama uplift in late Neogene time. Science, 217(4557): 350–352, doi: 10.1126/science.217.4557.350

Kuhnt W, Holbourn A, Hall R, et al. 2004. Neogene history of the Indonesian throughflow. In: Clift P, Kuhnt W, Wang Pinxian, Hayes D, eds. Continent-Ocean Interactions within East Asian Marginal Seas. Washington, DC, USA: American Geophysical Union, 299–320.

Li Hu, Wang Yingmin, Zhu Weilin, et al. 2013. Seismic characteristics and processes of the Plio-Quaternary unidirectionally migrating channels and contourites in the northern slope of the South China Sea. Marine and Petroleum Geology, 43: 370–380, doi: 10.1016/j.marpetgeo.2012.12.010

Li Yufeng, Pu Renhai, Fan Xiaowei, et al. 2017a. Characteristics and genesis of the polygonal fault system in Beijiao Sag of the Qiongdongnan Basin, the Northern South China Sea. Geotectonica et Metallogenia (in Chinese), 41(5): 817–828

Li Yufeng, Pu Renhai, Qu Hongjun, et al. 2017b. The characteristics and genesis analysis of the mound at the top of Meishan Formation in the Beijiao Sag of the Qiongdongnan Basin. Haiyang Xuebao (in Chinese), 39(5): 89–102

Li Yufeng, Pu Renhai, Qu Hongjun, et al. 2018. Distribution of bottom current channels and mounds controlled by Paleo-Morphology in Mid-Miocene in Beijiao Sag of Qiongdongnan Basin. Geological Science and Technology Information (in Chinese), 37(2): 1–8

Liao Jihua, Xu Qiang, Chen Ying, et al. 2016. Sedimentary characteristics and genesis of the deepwater channel system in Zhujiang Formation of Baiyun-Liwan Sag. Earth Science (in Chinese), 41(6): 1041–1054

Liu Siqing, Zhang Cuimei, Sun Zhen, et al. 2016. Characteristics and significances of the geological boundary SB21 in the Zhujiang Formation of the Liwan Sag, Pearl River Mouth Basin. Earth Science (in Chinese), 41(3): 475–486

Ma Yubo, Wu Shiguo, Gu Mingfeng, et al. 2010. Seismic reflection characteristics and depositional model of carbonate platforms in Xisha sea area. Haiyang Xuebao (in Chinese), 32(4): 118–128

Masson D G, Harbitz C B, Wynn R B, et al. 2006. Submarine landslides: processes, triggers and hazard prediction. Philosophical Transactions of the Royal Society A Mathematical Physical and Engineering Sciences, 364(1845): 2009–2039, doi: 10.1098/rsta.2006.1810

Meng Xiangjun, Zhang Xunhua, Han Bo, et al. 2012. The geophysical characteristics of submarine mud volcano. Marine Geology Frontiers (in Chinese), 28(12): 6–9, 45

Pu Renhai, Zhong Hongli, Zhang Yunlong. 2013. Preliminary study on the effects of Permian volcanism on the Tahe Ordovician oil pools in Tarim Basin. Marine and Petroleum Geology, 44: 13–20, doi: 10.1016/j.marpetgeo.2013.03.003

Ru K, Pigott J D. 1986. Episodic rifting and subsidence in the South China Sea. AAPG Bulletin, 70(9): 1136–1155

Shao Lei, Cui Yuchi, Qiao Peijun, et al. 2017. Sea-level changes and carbonate platform evolution of the Xisha Islands (South China Sea) since the early Miocene. Palaeogeography, Palaeoclimatology, Palaeoecology, 485: 504–516, doi: 10.1016/j.palaeo.2017.07.006

Shao Lei, Li Xuejie, Geng Jianhua, et al. 2007. Deep water bottom current deposition in the northern South China Sea. Science in China Series D: Earth Sciences, 50(7): 1060–1066, doi: 10.1007/s11430-007-0015-y

Stow Dorrik A V, Armishaw Julie E, Holmes Richard. 2002. Holocene contourite sand sheet on the Barra Fan slope, NW Hebridean margin. Geological Society London Memoirs, 22(1): 99–119, doi: 10.1144/GSL.MEM.2002.022.01.09

Stuart J Y, Huuse M. 2012. 3D seismic geomorphology of a large Plio-Pleistocene delta—'Bright spots' and contourites in the South-

ern North Sea. Marine and Petroleum Geology, 38(1): 143–157, doi: 10.1016/j.marpetgeo.2012.06.003

Sun Qiliang, Cartwright J, Lüdmann T, et al. 2017. Three-dimensional seismic characterization of a complex sediment drift in the South China Sea: Evidence for unsteady flow regime. Sedimentology, 64(3): 832–853, doi: 10.1111/sed.12330

Sun Qiliang, Cartwright J, Wu Shiguo, et al. 2016. Submarine erosional troughs in the northern South China Sea: Evidence for Early Miocene deepwater circulation and paleoceanographic change. Marine and Petroleum Geology, 77: 75–91, doi: 10.1016/j.marpetgeo.2016.06.005

Tian Jie, Wu Shiguo, Lv Fuliang, et al. 2015. Middle Miocene mound-shaped sediment packages on the slope of the Xisha carbonate platforms, South China Sea: Combined result of gravity flow and bottom current. Deep Sea Research Part Ⅱ: Topical Studies in Oceanography, 122(2015): 172–184

Tsuchi R. 1997. Marine climatic responses to Neogene tectonics of the Pacific Ocean seaways. Tectonophysics, 281(1–2): 113–124, doi: 10.1016/S0040-1951(97)00163-7

Wang Chao, Lu Yongchao, Du Xuebin, et al. 2015. Developmental pattern and genetic background of carbonate platform margin reef complexes in deep-water area in western South China Sea. Oil Geophysical Prospecting (in Chinese), 50(6): 1179–1189

Wilson J L. 1975. Carbonate Facies in Geologic History. New York: Springer-Verlag Press, 451–471.

Wu Shiguo, Yang Zhen, Wang Dawei, et al. 2014. Architecture, development and geological control of the Xisha carbonate platforms, northwestern South China Sea. Marine Geology, 350: 71–83, doi: 10.1016/j.margeo.2013.12.016

Wu Shiguo, Yuan Shengqiang, Zhang Gongcheng, et al. 2009. Seismic characteristics of a reef carbonate reservoir and implications for hydrocarbon exploration in deepwater of the Qiongdongnan Basin, northern South China Sea. Marine and Petroleum Geology, 26(6): 817–823, doi: 10.1016/j.marpetgeo.2008.04.008

Xie Xinong, Müller R D, Li Sitian, et al. 2006. Origin of anomalous subsidence along the northern south china sea margin and its relationship to dynamic topography. Marine and Petroleum Geology, 23(7): 745–765, doi: 10.1016/j.marpetgeo.2006.03.004

Xue Huijie, Chai Fei, Neal Pettigrew, et al. 2004. Kuroshio intrusion and the circulation in the South China Sea. Journal of Geophysical Research, 109(C2): C02017

Yang Bo, Zhang Changmin, Li Shaohua, et al. 2014. Seismic facies analysis and geological interpretation of large-scale mounds in Pearl River Mouth Basin. Acta Petrolei Sinica (in Chinese), 35(1): 37–49

Yi Wanshun, Deng Yantao, Di Bangrang. 2012. Discussion on the genesis of domal reflections at the uplift zone of the southern Qiongdongnan Basin. Geophysical Prospecting for Petroleum (in Chinese), 51(2): 199–203

Zhang Bin, Wang Pujun, Zhang Gongcheng, et al. 2013. Cenozoic volcanic rocks in the Pearl River Mouth and Southeast Hainan Basins of South China Sea and their implications for petroleum geology. Petroleum Exploration and Development, 40(6): 704–713, doi: 10.1016/S1876-3804(13)60095-6

Zhang Gongcheng. 2010. Tectonic evolution of deepwater area of northern continental margin in South China Sea. Acta Petrolei Sinica (in Chinese), 31(4): 528–533, 541

Zhang Gongcheng, Liu Zhen, Mi Lijun, et al. 2009. Sedimentary evolution of Paleogene series in deep water area of Zhujiangkou and Qiongdongnan Basin. Acta Sedimentologica Sinica (in Chinese), 27(4): 632–641

Zhang Yonggui, Song Zaichao, Zhou Xiaojin, et al. 2011. Identification of reef in Miocene, South of Qiongdongnan Basin. Petroleum Geology & Experiment (in Chinese), 33(3): 307–309, 313

Zhao Tianliang, Pu Renhai, Qu Hongjun, et al. 2013. An origin discussion of mound-shaped reflections in Miocene, southern Qiongdongnan Basin. Haiyang Xuebao (in Chinese), 35(4): 112–120

Zhu Mangzheng, Graham S, Pang Xiong, et al. 2010. Characteristics of migrating submarine canyons from the middle Miocene to present: Implications for paleoceanographic circulation, northern South China Sea. Marine and Petroleum Geology, 27(1): 307–319, doi: 10.1016/j.marpetgeo.2009.05.005